

Toward a Unified Model Explaining Heterogeneous Ziegler–Natta Catalysis

Raffaele Credendino,[†] Dario Liguori,[‡] Zhiqiang Fan,[§] Giampiero Morini,[‡] and Luigi Cavallo^{*,†}

[†]King Abdullah University of Science and Technology (KAUST), Physical Sciences and Engineering Division, Kaust Catalysis Center, Thuwal 23955-6900, Saudi Arabia

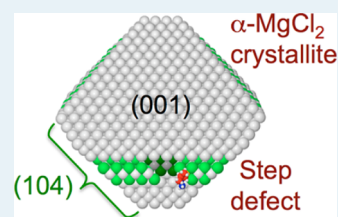
[‡]LyondellBasell Polyolefins, G. Natta Research Center, Piazzale G. Donegani 12, 44100 Ferrara, Italy

[§]Department of Polymer Science and Engineering, MOE Key Laboratory of Macromolecular Synthesis and Functionalization, Zhejiang University, Hangzhou 310027, China

S Supporting Information

ABSTRACT: We propose a model for MgCl₂-supported Ziegler–Natta catalysts, which is capable to reconcile the discrepancies emerging in the last 20 years, in which attempts have been made to rationalize experimental data by molecular models. We show that step defects on the thermodynamically more stable (104) facet of MgCl₂ can lead to sites for strong TiCl₄ adsorption. The corresponding Ti-active site is stereoselective, and its stereoselectivity can be enhanced by coordination of Al-alkyls or Lewis bases in the close proximity. The surface energy of the step defected (104) MgCl₂ facet is clearly lower than that of the well accepted (110) facet.

KEYWORDS: heterogeneous catalysis, stereoselective polymerization, Ziegler–Natta catalysis, isotactic polypropylene, DFT calculations



Despite the economic relevance of polyolefin commodities, with a volume in the order of 10⁶ tons/year and a billion dollar market, the intimate nature of the active site of Ziegler–Natta (ZN) catalysts remains elusive. This limited knowledge is a consequence of the complex nature of ZN-catalysts, although four key ingredients only compose industrial catalysts. They are the inert MgCl₂ support; the catalytically active TiCl₄ adsorbed on the MgCl₂ surfaces; an Al-alkyl, typically AlEt₃, to activate the adsorbed TiCl₄; and a Lewis base, either monodentate as benzoates or bidentate as siloxanes, phthalates, 1,3-diethers and succinates, to tune catalytic behavior and to increase the amount and stereoregularity of the produced polypropylene.^{1–4}

The main difficulty in composing this four-piece puzzle is in the uncertainty about the MgCl₂ surface(s) hosting the catalytically active Ti-species. Indeed, solving this issue would allow proposing reasonable models, because we have a reasonable knowledge of the local geometry that should be assumed by the catalytically active Ti-species. In this regard, there is consensus that the dominant surface in MgCl₂ crystallites, the basal (001) surface corresponding to a plane of Cl atoms, see Figure 1, cannot adsorb TiCl₄. However, there is not agreement on which lateral facet hosts the catalytically active Ti-species. The only convergence is on the nature of the two possible facets: the more stable (104)-facet, presenting penta-coordinated Mg atoms, or the less stable (110)-facet, presenting tetra-coordinated Mg atoms,^{5–18} see Figure 1.

Early models, based on the similarity between the (100) and the (110)-facets of MgCl₂ and TiCl₃ monolayers, suggested that the more stable (104)-facet could host dimeric Ti₂Cl₈ species, with the benefit that the environment around the Ti atoms would mimic the stereoselective sites proposed for TiCl₃.^{19–23} In this scheme, the (110)-facet is not stereo-

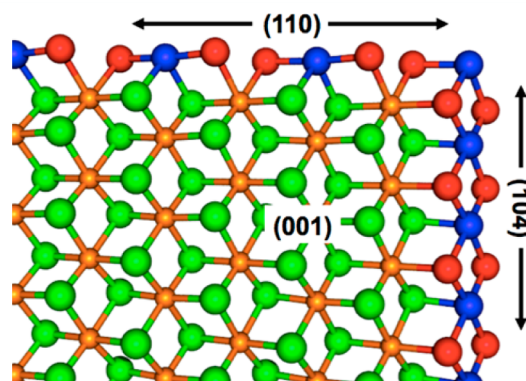


Figure 1. MgCl₂ crystallite showing the basal (001) and the lateral (104) and (110)-facets.

selective, and Lewis bases would poison the (110)-facet preventing TiCl₄ adsorption.²⁴ This scheme dominated the literature for about 20 years since the discovery of supported ZN-catalysts. More recently, severe criticism has questioned this scheme. First, a series of static and dynamic DFT calculations indicated that TiCl₄ adsorption on the (104)-facet is weak, and formation of dimeric Ti₂Cl₈ is practically impossible.^{5,6,8,12,25} Differently, TiCl₄ was found to adsorb quite strongly on the (110)-facet. Second, experiments indicated that the Lewis base strongly influences the stereoregularity of the isotactic polypropylene,^{26–29} which implies

Received: May 22, 2015

Revised: July 21, 2015

Published: August 12, 2015

that the Lewis base can coordinate close to the active Ti-species and that it can actively participate in the stereocontrol event. However, models of the two surfaces indicated that there is no simple way to place a Lewis base in the proximity of the Ti-center on the (104)-facet, whereas it is simple to imagine a stereoselective role for the Lewis base on the (110)-facet.^{10,11,15}

On the basis of this evidence, the (104)-facet was basically abandoned in favor of the (110)-facet, currently considered as the most likely facet active in catalysis.

Unfortunately, even this scenario cannot unify all the experimental knowledge.^{18,30–41} The most striking incongruence is the experimental evidence that synthesizing the MgCl_2 support in the presence of diisobutyl phthalate or ethyl benzoate leads to the formation of crystallites presenting both 120° and 90° edge angles,⁴² the latter indicating the formation of crystallites presenting both the (104)- and (110)-facets. Subsequent treatment with TiCl_4 generates a catalyst that polymerizes propylene on all the lateral facets of each crystallite.⁴³ This clearly indicates that polymer can be produced on both the (104)- and (110)-facets, at odds with the evidence that TiCl_4 cannot adsorb on the (104)-facet, and that there is no model explaining the stereoselective role of the Lewis bases on the (104)-facet.

On the basis of DFT calculations,⁴⁴ we propose a model reconciling all these incongruences. In line with recent efforts focusing on determining low energy defected MgCl_2 surfaces,^{13,45} we propose a new low energy defect on the (104)-facet that can strongly coordinate TiCl_4 . The defect we propose allows rationalizing easily the stereoselective role of the Lewis bases also on the (104)-facet. Combined with previous knowledge on the (110)-facet, our results provide a conceptual scheme explaining almost all the knowledge in the field.⁴⁶

Starting from bulk MgCl_2 , we imagined different fragmentation modes generating perfect or step-defected (104)-facets, see Figure 2. While the perfect (104)-facet corresponds to a perfectly flat surface, the considered defected facet corresponds to have a fragmentation event generating a symmetric step defect on the two surfaces. Comparison between the fragmentation energy of the bulk into the perfect or into step-defected (104)-facets of different size converges in the single step-defect costing only 7.1 kcal/mol, details on the calculation of this value can be found in the Supporting Information. This value is comparable to the experimental values for the step energy on the Ag(111)- or Cu(111)-facets, around 6 kcal/mol per atomic distance.^{47,48} Analysis of the step-defected surface shows that the defect corresponds to a junction between the (104)- and the (110)-facets, with a local environment capable to host TiCl_4 almost epitaxially.

To relate the stability of the step-defected (104)-facet to that of the perfect (104)- and (110)-facets, we calculated the surface energy, E_{surf} of the perfect (104)- and (110)-facets and that of the step-defected (104) facet presenting a variable amount of isolated defects, see the Supporting Information for details. In agreement with previous work,¹⁷ we found that the perfect (104)-facet, with an E_{surf} of 0.410 J/m², is remarkably more stable than the perfect (110)-facet, with an E_{surf} of 0.722 J/m², see Table 1. Interestingly, the E_{surf} of the (104)-facet presenting 10%, 20%, and 30% of isolated step-defects is only 0.429, 0.448, and 0.466 J/m², indicating that even a highly defected (104)-facet is clearly more stable than the well accepted (110)-facet. Inclusion of a dispersion term modifies the overall E_{surf} values, but the trend is the same. Considering that preparation of MgCl_2 supports is usually performed under rather drastic

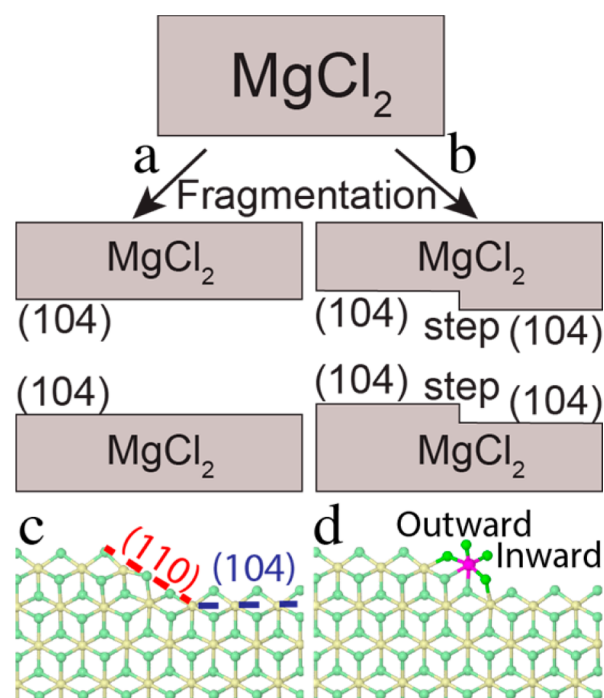


Figure 2. Fragmentation of MgCl_2 creating: (a) perfect (104)-facets; (b) (104)-facets presenting a step-defect. (c) geometry of the step-defect on the (104)-facet; (d) TiCl_4 adsorbed on the (104) step-defect.

Table 1. Surface Energy, E_{surf} in J/m², of Perfect (104)- and (110)-facets, and of Defected (104)-Facets Presenting a Variable Amount of Step-Defects

	% of defects	E_{surf}^a	E_{surf}^b
(104)	0	0.410	0.524
(104)	10	0.429	0.539
(104)	20	0.448	0.561
(104)	30	0.466	0.583
(110)	0	0.722	0.912

^aNo dispersion term included in the calculations. ^bAn empirical dispersion term is included in the calculations.

conditions, these results indicate that defected surfaces can have a relevant role in Ziegler–Natta catalysis. At this point, we moved to investigate TiCl_4 adsorption on the (104) step-defect.

According to calculations, TiCl_4 can be accommodated on the (104) step-defect with an overall binding energy of −12.5 kcal/mol, see Figure 2d. This value is much higher than that calculated for TiCl_4 adsorption on the perfect (104)-facet, only −2.8 kcal/mol, and it is comparable to that calculated for TiCl_4 adsorption on the perfect (110)-facet, −13.9 kcal/mol. Inclusion of dispersion interaction increases these values to −26.8, −12.5, and −25.5 kcal/mol for the (104) step-defect, and for the perfect (104)- and (110)-facets, respectively. Consistent with previous work,^{5,6,8,12,25} these numbers indicate that TiCl_4 cannot coordinate on the perfect (104)-facet when a disfavorable entropic penalty is considered, whereas strong coordination on the (104) step-defect or on the (110)-facet is possible also on a free-energy level. The good binding of TiCl_4 on the (104) step-defect and on the (110)-facet results from having octahedral coordination around the Ti-center, with the slightly stronger coordination of TiCl_4 on the (110) surface probably due to a stronger interaction of the coordinated

chlorine atoms of TiCl_4 with two tetracoordinated Mg atoms, see Figure S1, while TiCl_4 coordination on the (104) step-defect involves one tetracoordinated and one pentacoordinated Mg atom, see Figure 2d. Nevertheless, the main conclusion is that a step-defect on the more stable (104) surface is energetically feasible and can adsorb TiCl_4 as strong as the (110) facet.

At this point, we investigated chain growth, corresponding to propene insertion into the Ti-isobutyl bond (the isobutyl group is used to mimic a polymer chain), at a Ti-center adsorbed on the (104) step-defect. For the sake of simplicity, in all the calculations the configuration of the chiral Ti-center is Λ , and we considered insertion with the chain at both the inward and outward positions, see Figure 2.⁴⁶ In both cases, we located the transition state for primary and secondary insertion of the *re* and *si* enantiofaces of propene. A cluster model was used to investigate a larger number of cases, whereas a periodic boundary condition model was used to validate the cluster model and to investigate the impact of an industrially used Lewis base, 9,9-bis(methoxymethyl)-9*H*-fluorene (BMF).

According to calculations using the cluster model, primary insertion on the resulting catalytic site is not stereoselective if the growing chain is in the outward coordination position, with a $\Delta E_{\text{Stereo}}^\ddagger$ of only +0.1 kcal/mol, see Table 2, while it is slightly

Table 2. Stereo- and Regioselectivity of the Catalytic Sites with Nothing, AlEt_3 , or AlEt_2Cl Coordinated Next to the Ti-Center^a

nearby species		$\Delta E_{\text{Stereo}}^\ddagger$	$\Delta E_{\text{Regio}}^\ddagger$
cluster model			
outward	none	0.1	1.2
inward	none	1.2	1.1
outward	AlEt_3	0.9	1.4
inward	AlEt_3	1.2	1.1
outward	AlEt_2Cl	0.9	1.2
inward	AlEt_2Cl	1.4	1.3
nearby species		$\Delta E_{\text{Stereo}}^\ddagger$	$\Delta E_{\text{Regio}}^\ddagger$
periodic model			
outward	none	0.4	5.3
inward	none	3.9	5.9
outward	AlEt_3	2.2	6.0
outward	BMF	5.8	6.1

^a $\Delta E_{\text{Stereo}}^\ddagger$ and $\Delta E_{\text{Regio}}^\ddagger$ (in kcal/mol) correspond to the energy difference between the transition state for *re*- and *si*-propene primary insertion into the Ti-isobutyl bond, $\Delta E_{\text{Stereo}}^\ddagger$, and for the best secondary versus the best primary transition state for propene insertion into the Ti-isobutyl bond, $\Delta E_{\text{Regio}}^\ddagger$.

stereoselective if the growing chain is in the inward coordination position, with a $\Delta E_{\text{Stereo}}^\ddagger$ of +1.2 kcal/mol. Both catalytic sites are scarcely regioselective, with a $\Delta E_{\text{Regio}}^\ddagger$ around 1 kcal/mol. This result is expected, because no steric hindrance is restricting the conformational space available to the outward growing chain, while only the chlorine atom, indicated by a star in Figure 3, is somewhat restricting the conformational space available to the inward growing chain.

Next we investigated the impact of AlEt_3 and AlEt_2Cl on regio- and stereoselectivity, through their coordination in the proximity of the Ti atom, as shown in Figure 3. AlEt_3 is the compound mostly used to activate the adsorbed TiCl_4 species, whereas AlEt_2Cl is the Al-alkyl species resulting from the activation event. First, we checked that both these Al-alkyls

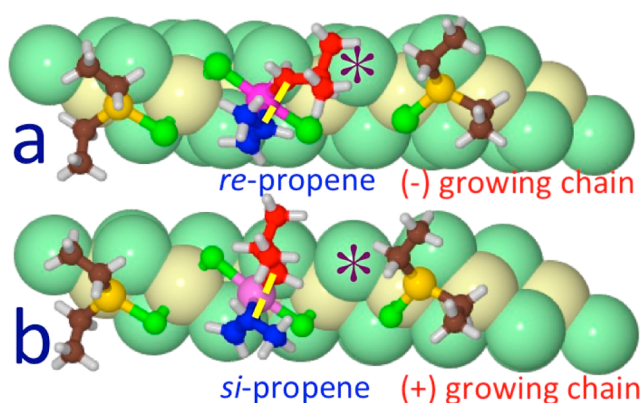


Figure 3. Models of the transition states for primary propene insertion with the growing chain in the inward coordination site. (a) Higher energy transition state, disfavored by steric interaction between the growing chain and the Cl atom marked by a star; (b) favored transition state. MgCl_2 in CPK, Ti-active site, propene, growing chain, AlEt_2Cl in ball and stick.

strongly coordinate on the perfect (104)-facet, which would infer strong coordination also in proximity of the step-defect. Gratifyingly, we calculated adsorption energies of 12.5 and 19.9 kcal/mol for AlEt_3 and AlEt_2Cl on a perfect (104)-facet, which is a good result considering that DFT is known to underestimate Al-alkyl dimerization energies.⁴⁹ Indeed, it ensures Al-alkyls adsorption to the MgCl_2 surface, considering that the experimental AlMe_3 and AlCl_3 dimerization energy is only 10 and 15 kcal/mol per AlMe_3 or AlCl_3 unit.^{50,51} Once strong coordination of the Al-alkyl species was confirmed, we investigated again stereo and regioselectivity of propene insertion. The numbers reported in Table 2 clearly indicate that the presence of the Al-alkyls increases the stereoselectivity of primary propene insertion, particularly when the growing chain is in the less hindered outward position, with $\Delta E_{\text{Stereo}}^\ddagger$ approaching 1 kcal/mol. A less-relevant impact of the Al-alkyls is instead calculated when the growing chain is in the already somewhat stereoselective inward position. Further, with both Al-alkyls primary propene insertion remains favored, with $\Delta E_{\text{Regio}}^\ddagger$ always above 1 kcal/mol. In short, TiCl_4 adsorption on a low energy (104) step-defect, with the near unsaturated Mg atoms decorated with Al-alkyls, can yield a moderately stereoselective site, in agreement with the experiments. Test calculations via single-point energy evaluations with the hybrid PBE1PBE functionals, among the best performing functionals in reproducing CCSD(T) barriers for olefin insertion and for β -H elimination in early transition metals,⁵² indicates that switching from a GGA to a HGGA functional changes somehow the value of $\Delta E_{\text{Stereo}}^\ddagger$ and $\Delta E_{\text{Regio}}^\ddagger$ but the overall conclusions remain the same, see the SI.

To further validate these conclusions, reached with a relatively small cluster, we performed additional calculations using a periodic model composed of three MgCl_2 monolayers, with the central monolayer hosting the defect and the active site (for further information see the SI). When we focused on the naked active site, the results using the periodic model are in line with those achieved with the cluster model, with a reinforcement of stereoselectivity when the growing chain is inward coordinated, due to clashes with the nearby MgCl_2 monolayer. As a further test, we calculated the regio- and stereoselectivity of the less-selective active site, with the chain in the outward position, in the presence of AlEt_3 and the BMF

Lewis base. Consistent with the results achieved with the cluster model, the presence of AlEt₃ molecules flanking the active site improves stereoselectivity. The presence of bulkier BMF molecules reinforcing this trend, again in agreement with the experiments.^{26,28}

In summary, TiCl₄ on (104)-facets presenting low-energy step-defects can complement the already known site corresponding to TiCl₄ on the perfect (110)-facet to explain basically all the available knowledge in ZN-catalysis. In fact, they are both potential sites for strong coordination of TiCl₄, and exactly the same mechanism, coordination of an Al-alkyl or a Lewis base in the proximity of the active Ti-center, can be used to confer stereoselectivity to the otherwise poorly stereoselective site. This unified mechanism is a remarkable advance in the field, because it rationalizes formation of isotactic polymer independently from the exposed facet as well as the shape and the angles between the edges of MgCl₂ crystallites. Further, it suggests that efforts should be made to locate other low energy defects that can host a Ti-active species whose stereoselectivity can be improved by the presence of Lewis bases.

■ ASSOCIATED CONTENT

📄 Supporting Information

The Supporting Information is available free of charge on the ACS Publications website at DOI: 10.1021/acscatal.5b01076.

Computational details, coordinates, and energy of all the minimum energy discussed in the text (PDF)

■ AUTHOR INFORMATION

Corresponding Author

*E-mail: luigi.cavallo@kaust.edu.sa.

Notes

The authors declare no competing financial interest.

■ ACKNOWLEDGMENTS

We thank ENEA (www.enea.it) and the HPC team for support and for using ENEA-GRID and the HPC facilities CRESCO (www.cresco.enea.it) Portici (Naples), Italy. The authors would like to dedicate this manuscript to the memory of Prof. Adolfo Zambelli, one of the fathers of stereoselective propene polymerization. The authors would like to dedicate this manuscript to the memory of Prof. Adolfo Zambelli, one of the fathers of stereoselective propene polymerization.

■ REFERENCES

- (1) Moore, E. P., Jr. *Polypropylene Handbook: Polymerization, Characterization, Properties, Applications*; Hanser Publishers: Munich, 1996.
- (2) Natta, G. In *Nobel Lectures in Chemistry, 1963–1970*; Elsevier: Amsterdam, 1972; p 27.
- (3) Ziegler, K. In *Nobel Lectures in Chemistry, 1963–1970*; Elsevier: Amsterdam, 1972; p 6.
- (4) Resconi, L.; Cavallo, L.; Fait, A.; Piemontesi, F. *Chem. Rev.* **2000**, *100*, 1253.
- (5) Seth, M.; Margl, P. M.; Ziegler, T. *Macromolecules* **2002**, *35*, 7815.
- (6) Boero, M.; Parrinello, M.; Weiss, H.; Hüffer, S. *J. Phys. Chem. A* **2001**, *105*, 5096.
- (7) D'Amore, M.; Credendino, R.; Budzelaar, P. H. M.; Causa, M.; Busico, V. *J. Catal.* **2012**, *286*, 103.
- (8) Boero, M.; Parrinello, M.; Hüffer, S.; Weiss, H. *J. Am. Chem. Soc.* **2000**, *122*, 501.

- (9) Stukalov, D. V.; Zilberberg, I. L.; Zakharov, V. A. *Macromolecules* **2009**, *42*, 8165.
- (10) Correa, A.; Piemontesi, F.; Morini, G.; Cavallo, L. *Macromolecules* **2007**, *40*, 9181.
- (11) Taniike, T.; Terano, M. *Macromol. Rapid Commun.* **2007**, *28*, 1918.
- (12) Monaco, G.; Toto, M.; Guerra, G.; Corradini, P.; Cavallo, L. *Macromolecules* **2000**, *33*, 8953.
- (13) Kuklin, M. S.; Bazhenov, A. S.; Denifl, P.; Leinonen, T.; Linnolahti, M.; Pakkanen, T. A. *Surf. Sci.* **2015**, *635*, 5.
- (14) Credendino, R.; Pater, J. T. M.; Liguori, D.; Morini, G.; Cavallo, L. *J. Phys. Chem. C* **2012**, *116*, 22980.
- (15) Correa, A.; Credendino, R.; Pater, J. T. M.; Morini, G.; Cavallo, L. *Macromolecules* **2012**, *45*, 3695.
- (16) Credendino, R.; Pater, J. T. M.; Correa, A.; Morini, G.; Cavallo, L. *J. Phys. Chem. C* **2011**, *115*, 13322.
- (17) Credendino, R.; Busico, V.; Causa, M.; Barone, V.; Budzelaar, P. H. M.; Zicovich-Wilson, C. *Phys. Chem. Chem. Phys.* **2009**, *11*, 6525.
- (18) Busico, V.; Causa, M.; Cipullo, R.; Credendino, R.; Cutillo, F.; Friederichs, N.; Lamanna, R.; Segre, A.; VanAxelCastelli, V. *J. Phys. Chem. C* **2008**, *112*, 1081.
- (19) Corradini, P.; Barone, V.; Fusco, R.; Guerra, G. *Eur. Polym. J.* **1979**, *15*, 1133.
- (20) Corradini, P.; Guerra, G.; Fusco, R.; Barone, V. *Eur. Polym. J.* **1980**, *16*, 835.
- (21) Corradini, P.; Barone, V.; Guerra, G. *Macromolecules* **1982**, *15*, 1242.
- (22) Corradini, P.; Barone, V.; Fusco, R.; Guerra, G. *Gazz. Chim. Ital.* **1983**, *113*, 601.
- (23) Corradini, P.; Guerra, G.; Barone, V. *Eur. Polym. J.* **1984**, *20*, 1177.
- (24) Toto, M.; Morini, G.; Guerra, G.; Corradini, P.; Cavallo, L. *Macromolecules* **2000**, *33*, 1134.
- (25) Boero, M.; Parrinello, M.; Terakura, K. *J. Am. Chem. Soc.* **1998**, *120*, 2746.
- (26) Chadwick, J. C.; Morini, G.; Balbontin, G.; Mingozi, I.; Albizzati, E.; Sudmeijer, O. *Macromol. Chem. Phys.* **1997**, *198*, 1181.
- (27) Sacchi, M. C.; Forlini, F.; Tritto, I.; Locatelli, P.; Morini, G.; Noristi, L.; Albizzati, E. *Macromolecules* **1996**, *29*, 3341.
- (28) Morini, G.; Albizzati, E.; Balbontin, G.; Mingozi, I.; Sacchi, M. C.; Forlini, F.; Tritto, I. *Macromolecules* **1996**, *29*, 5770.
- (29) Sacchi, M. C.; Forlini, F.; Tritto, I.; Locatelli, P.; Morini, G.; Baruzzi, G.; Albizzati, E. *Macromol. Symp.* **1995**, *89*, 91.
- (30) Albizzati, E.; Giannini, U.; Collina, G.; Noristi, L.; Resconi, L. In *Polypropylene Handbook*; Moore, E. P., Ed.; Hanser Publishers: Munich, 1996; p 11.
- (31) Brant, P.; Specia, A. N.; Johnston, D. C. *J. Catal.* **1988**, *113*, 250.
- (32) Kashiwa, N.; Yoshitake, J. *Makromol. Chem.* **1984**, *185*, 1133.
- (33) Paukkeri, R.; Lehtinen, A. *Polymer* **1993**, *34*, 4083.
- (34) Randall, J. C. *Macromolecules* **1997**, *30*, 803.
- (35) Busico, V.; Cipullo, R.; Monaco, G.; Talarico, G.; Vacatello, M.; Chadwick, J. C.; Segre, A. L.; Sudmeijer, O. *Macromolecules* **1999**, *32*, 4173.
- (36) Potapov, A. G.; Kriventsov, V. V.; Kochubey, D. I.; Bukatov, G. D.; Zakharov, V. A. *Macromol. Chem. Phys.* **1997**, *198*, 3477.
- (37) Jensen, V. R.; Børve, K. J.; Ystenes, M. *J. Am. Chem. Soc.* **1995**, *117*, 4109.
- (38) Sakai, S. *Trends in Physical Chemistry* **1997**, *6*, 235.
- (39) Puhakka, E.; Pakkanen, T. T.; Pakkanen, T. A. *J. Mol. Catal. A: Chem.* **1997**, *120*, 143.
- (40) Stukalov, D. V.; Zakharov, V. A.; Potapov, A. G.; Bukatov, G. D. *J. Catal.* **2009**, *266*, 39.
- (41) Martinsky, C.; Minot, C.; Ricart, J. M. *Surf. Sci.* **2001**, *490*, 237.
- (42) Mori, H.; Sawada, M.; Higuchi, T.; Hasebe, K.; Otsuka, N.; Terano, M. *Macromol. Rapid Commun.* **1999**, *20*, 245.
- (43) Andoni, A.; Chadwick, J. C.; Niemantsverdriet, H. J. W.; Thüne, P. C. *J. Catal.* **2008**, *257*, 81.
- (44) Calculations using a periodic model were performed with the CP2K package using a triple- ζ basis set and the PBE functional.

Calculations of the active site with the cluster model were performed with Gaussian09 package, at the same level of theory.

(45) Bazhenov, A.; Linnolahti, M.; Pakkanen, T. A.; Denifl, P.; Leinonen, T. *J. Phys. Chem. C* **2014**, *118*, 4791.

(46) Details on the DFT calculations, on the models composition, and on the definition of outward and inward growing chain can be found in the [Supporting Information](#).

(47) Schlöber, D. C.; Verheij, L. K.; Rosenfeld, G.; Comsa, G. *Phys. Rev. Lett.* **1999**, *82*, 3843–3846.

(48) Morgenstern, K.; Rosenfeld, G.; Laegsgaard, E.; Besen-Bacher, F.; Comsa, G. *Phys. Rev. Lett.* **1998**, *80*, 556–559.

(49) Willis, B. G.; Jensen, K. F. *J. Phys. Chem. A* **1998**, *102*, 2613.

(50) Henrickson, C. H.; Eyman, D. P. *Inorg. Chem.* **1967**, *6*, 1461.

(51) Wade, K. *J. Chem. Educ.* **1972**, *49*, 502.

(52) Ehm, C.; Budzelaar, P. H. M.; Busico, V. *J. Organomet. Chem.* **2015**, *775*, 39.